Probability of Convectively Induced Turbulence Associated with Geostationary Satellite–Inferred Cloud-Top Cooling

SARAH A. MONETTE AND JUSTIN M. SIEGLAFF

Cooperative Institute for Meteorological Satellite Studies, University of Wisconsin—Madison, Madison, Wisconsin

(Manuscript received 22 May 2013, in final form 23 October 2013)

ABSTRACT

The probability of turbulence in the region of identified cloud-top cooling (CTC) from a satellite-based algorithm is calculated. It is found that the overall turbulence probability is low, with only 3.93% of 738 Boeing 737s and 757s experiencing light or greater turbulence. Predicting the probability of turbulence is done using a Bayesian scheme. This prediction scheme relies on the CTC magnitude as well as the relationship between the CTC and aircraft. At higher CTC magnitudes [$\leq -16\,\mathrm{K}\,(15\,\mathrm{min})^{-1}$], turbulence is more common, with the conditional probability of turbulence exceeding the conditional probability of no turbulence. Aircraft with flight levels that are less than 8000 ft (~2440 m) above the cloud height also have a higher conditional probability of turbulence than no turbulence. Overall, the Bayesian scheme is found to be more skillful when compared with use of climatological information alone.

1. Introduction

Convectively induced turbulence (CIT) is a documented in-flight aviation hazard (Hamilton and Proctor 2002). Thunderstorms account for most air traffic delays in the United States (Kaplan et al. 2005; Murray 2002; Mecikalski et al. 2007), but the developmental stages of thunderstorms can also be a cause of CIT, sometimes unseen by pilots. For example, on 3 August 2009, a Continental Airlines Boeing 767-200 encountered turbulence as a result of ''the flight crew's inadvertent flight through the top of a convective updraft,'' even though the pilot was able to see ground lights minutes before (National Transportation Safety Board incident DCA09IA071; for brief and full narratives of the incident see online at http://www.ntsb.gov/aviationquery/brief.aspx?ev_id=20090810X21314&key=1).

Convective updrafts can be inferred by monitoring cooling trends of infrared (IR) window brightness temperatures (BT) from geostationary satellites [e.g., Geostationary Operational Environmental Satellite (GOES)]. One such approach, the University of Wisconsin cloud-top cooling (UW-CTC; Sieglaff et al. 2011) algorithm, is shown in Fig. 1. The UW-CTC algorithm diagnosed a rapidly cooling convective cloud just north of Hispaniola coincident with the Continental flight. The objective of this analysis is to predict light or greater turbulence for aircraft flying within/over a cloud that currently has a measurable UW-CTC rate. This paper identifies the probability of experiencing CIT in the region of these clouds and uses attributes of the UW-CTC algorithm to better predict the probability of CIT. In this paper, CIT will refer to both in-cloud and out-of-cloud turbulence.

2. Data

a. Cloud-top cooling algorithm

The UW-CTC algorithm that is used in this analysis uses an approach called box averaging (Sieglaff et al. 2011). Centered on each *GOES-East* pixel is a box of 7×7 pixels that is used to compute a box-average IR BT, excluding pixels deemed clear or fog by the GOES-R Advanced Baseline Imager (ABI) cloud-typing algorithm that is described in Pavolonis (2010). At least 5% of the box must be cloudy for consideration, allowing more than one pixel to contribute to the box-averaged IR BT. The domain for this analysis covers a region extending from 21° to 51°N and from 66° to 104°W.

Using the current and previous satellite scan times, the box-averaged IR BT fields are differenced (current − previous) to calculate the unfiltered CTC. This unfiltered

Corresponding author address: Sarah A. Monette, Cooperative Institute for Meteorological Satellite Studies, 1225 W. Dayton St., Madison, WI 53706.
E-mail: sarah.monette@ssec.wisc.edu

DOI: 10.1175/JAMC-D-13-0174.1

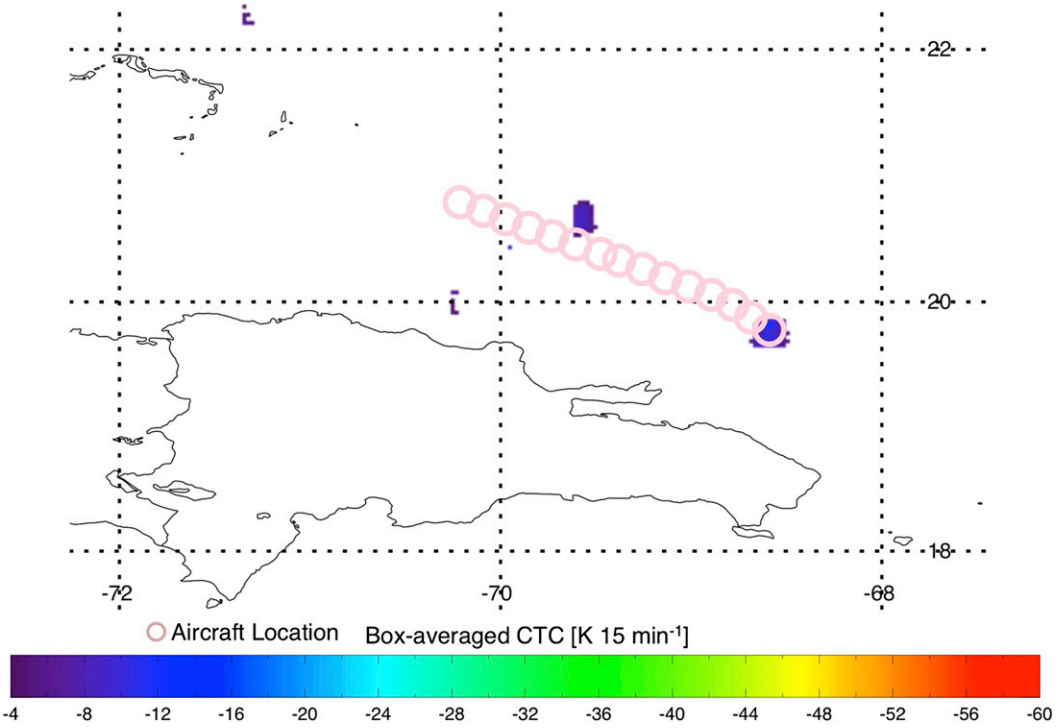

FIG. 1. CTC and Continental Airlines flight 128 track at 0802 UTC 3 Aug 2009. The plotted track is within ±7 min of the satellite scan time. Note the flight track over the colored CTC just north of Hispaniola's eastern point. The timing of this occurrence corresponds to the time that the Boeing 767-200 aircraft experienced turbulence.

CTC is normalized to a 15-min CTC rate to account for temporal inconsistencies in the GOES scan schedule. This unfiltered CTC rate can either represent horizontal movement (cold cloud moving into the box previously occupied by a warm cloud) or vertical growth (cloud remaining in the box and increasing in vertical extent). A series of tests are performed to remove false cooling that results from horizontal cloud advection, leaving only CTC signatures that are related to vertical cloud growth. These tests, as well as a full description of the CTC algorithm, can be found in Sieglaff et al. (2011). In addition, GOES visible optical depth (VOD; Walther and Heidinger 2012) has been incorporated into the UW-CTC algorithm to detect growing convection beneath regions of thin cirrus clouds during daytime hours. The introduction of GOES VOD to the UW-CTC algorithm has allowed for a higher number of storm identifications while increasing the UW-CTC algorithm skill (Sieglaff et al. 2013).

In addition to the UW-CTC algorithm, output from the GOES-R ABI cloud-height algorithm (ACHA) is also employed in this study. ACHA uses ancillary data, including surface information and a radiative transfer model, as well as data from numerical weather prediction models (see section 2c) to derive cloud-top height and pressure (Heidinger 2011).

b. Eddy dissipation rate turbulence observations

Eddy dissipation rate (EDR) values derive from vertical motions experienced by an aircraft and provide a quantitative measure of atmospheric turbulence intensity (Cornman et al. 1995, 2004a). The Research Applications Laboratory of the National Center for Atmospheric Research provided the EDR values that were used in this project. EDR values for aircraft above flight level 200 (20 000 ft in pressure altitude coordinates; 1 ft ≈ 0.3 m) and not ascending or descending [defined as 5000 ft $(15\ \text{min})^{-1}$] will be considered in this analysis. Pressure altitude is the altitude of a given value of atmospheric pressure according to the International Civil Aviation Organization (ICAO) standard atmosphere (Glickman 2000).

The dependent dataset used in this analysis includes EDR data from United Airlines (UAL) Boeing 737 and 757 aircraft from 2008 and Delta Airlines (DAL) Boeing 737 aircraft from 2010. In addition, EDR data from DAL Boeing 737 aircraft from 2011 will be used in an independent test of performance. EDR data are reported on a 0–1 scale, with UAL and DAL data being reported at intervals of 0.10 and 0.02 $\text{m}^{2/3}\,\text{s}^{-1}$, respectively.

EDR reporting strategies vary between UAL and DAL. EDR data from UAL are estimated by using

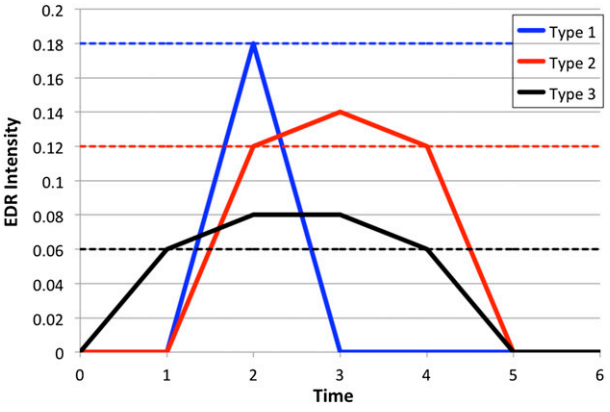

FIG. 2. Schematic illustrating the Delta Airlines EDR reporting triggering logic. Blue represents a type-1 report in which an EDR value greater than or equal to 0.18 is experienced. Red represents a type-2 report in which an EDR value greater than or equal to 0.12 is experienced for at least 3 out of the last 6 min. Black represents a type-3 report in which an EDR value greater than or equal to 0.06 is experienced for 4 out of the last 6 min.

vertical accelerometer data (Cornman et al. 2004b) and are reported every minute. DAL EDR values are calculated by using vertical wind data (Cornman et al. 2004b), and reporting relies on a triggering logic (Meymaris and Sharman 2013). A DAL EDR is reported every 15 min unless one of the following three types of minimum events occur:

1) in type 1, an EDR value of greater than or equal to 0.18 is experienced,
2) in type 2, an EDR value of greater than or equal to 0.12 is experienced for 3 of the last 6 min, and
3) in type 3, an EDR value of greater than or equal to 0.06 is experienced for 4 of the last 6 min.

A pictorial example of this type of EDR reporting, adapted from Meymaris and Sharman (2013), can be seen in Fig. 2. Although these data can be interpolated to 1-min temporal frequency, only noninterpolated data will be used in this analysis because lower EDR values (those less than $0.18\,m^{2/3}\,s^{-1}$) could be lost by the triggering logic if not experienced over a certain length of time.

Categorical (e.g., light or moderate) turbulence can be identified by using EDR thresholds. According to the International Civil Aviation Organization (2007), light or greater turbulence (LOGT) is observed when EDR values are greater than 0.1. A full comparison of EDR values with categorical turbulence using the ICAO standards can be found in Table 1. Another method for identifying categorical turbulence can be found by comparing EDR values with pilot reports (PIREPs) of turbulence. The turbulence-intensity criteria definition and numerical value assigned to each PIREP can be found in Schwartz (1996). According to Pearson and Sharman (2013), UAL and DAL EDR values are related to PIREP values by the equation EDR = 0.0138 (PIREP intensity)^2. Using the relationship between categorical turbulence and PIREP intensity in Table 2 [adapted from Schwartz (1996)], the EDR value for light turbulence is 0.055. Thus, EDR values greater than or equal to 0.10 (0.06) for UAL (DAL) are considered to be LOGT in this analysis, which is hereinafter referred to as the PIREP standard. A full comparison of EDR values with categorical turbulence for the PIREP standard can be found in Table 3.

TABLE 1. EDR value and corresponding turbulence category as based on the International Civil Aviation Organization (2007) standards.

EDR $\leq$ 0.1	No turbulence
0.1 $<$ EDR $<$ 0.4	Light turbulence
0.4 $<$ EDR $<$ 0.70	Moderate turbulence
EDR $\geq$ 0.70	Severe turbulence

c. *Numerical weather prediction models*

The GOES cloud products require data from numerical weather prediction (NWP) models—temperature and moisture profiles, to be specific. For 2010 and 2011 cases, 12-h forecasts from the 0.5°-resolution Global Forecast System NWP model are used, and the 2008 analysis relies on 0-h forecasts from the 1.0°-resolution Global Data Assimilation System NWP model. Since the NWP models are valid at 0000, 0600, 1200, and 1800 UTC, the forecasts valid prior to and after the analysis time are used as inputs into the GOES cloud-product computations.

3. Method

According to Sieglaff et al. (2011), the average movement of convective clouds is 5 km (5 min)$^{-1}$, with a standard deviation of 2 km (5 min)$^{-1}$. Therefore, a cloud with a movement speed that is 3 standard deviations above the mean has a speed of 11 km (5 min)$^{-1}$, or 2.2 km min^{-1}, the upper bound for this analysis. For an aircraft to have possibly flown though a cloud exhibiting a UW-CTC rate, its location must be within

TABLE 2. Turbulence category and corresponding PIREP intensity adapted from Schwartz (1996).

Categorical turbulence	PIREP intensity
Null	0
Light	2
Moderate	4
Severe	6

TABLE 3. EDR value and corresponding turbulence category for the PIREP standard as based on Pearson and Sharman (2013).

EDR ≤ 0.055	No turbulence
$0.055 <$ EDR < 0.22	Light turbulence
$0.22 <$ EDR < 0.50	Moderate turbulence
EDR ≥ 0.50	Severe turbulence

$2.2\,\mathrm{km\,min^{-1}} \times |\text{EDR report time} - \text{satellite scan time}|$ of the CTC location. This will be the radius of uncertainty. The prediction interval used is 7 min; one-half of the average time between *GOES-East* scans over the continental United States.

Because UAL EDRs are reported every minute (Cornman et al. 2004a), an aircraft could report an EDR up to 30 s after encountering a cloud exhibiting a UW-CTC rate. A Boeing 737-800 has a typical cruising speed of $0.785 \times$ Mach (see ''commercial airplanes—737-800 technical characteristics'' online at http://www.boeing.com/commercial/737family/pf/pf_800tech.html), or about $15.5\,\mathrm{km\,min^{-1}}$ (where Mach $1 = 330\,\mathrm{m\,s^{-1}}$; see ''Mach number'' online at http://www.grc.nasa.gov/WWW/k-12/airplane/mach.html).

A Bayesian scheme will be utilized to calculate the probability of CIT in the region of a CTC. According to Bayes's theorem, the probability of CIT is conditional on the features set **F**, which can be described by

$$P(C_{\text{turb}} \,|\, \mathbf{F}) = \frac{P(C_{\text{turb}})P(\mathbf{F} \,|\, C_{\text{turb}})}{P(\mathbf{F})}, \tag{1}$$

where $P(C_{\text{turb}} \,|\, \mathbf{F})$ is referred to as the ''posterior probability.'' The ''prior probability'' $P(C_{\text{turb}})$ is the probability assigned without knowledge of features. This is also referred to as the ''climatology,'' that is, the number of aircraft flights experiencing LOGT (C_{turb}) divided by all aircraft flights within the radius of uncertainty. The ''class-conditional probability'' $P(\mathbf{F} \,|\, C_{\text{turb}})$ is the probability of observing a set of features when experiencing LOGT, and $P(\mathbf{F})$ is the probability of observing a set of features independent of experienced turbulence (Kossin and Sitkowski 2009; Wilks 2006). By assuming that each feature within our feature set **F** is independent, $P(\mathbf{F} \,|\, C_{\text{turb}})$ can be rewritten as

$$P(\mathbf{F} \,|\, C_{\text{turb}}) = \prod_{i=1}^{N} P(F_i \,|\, C_{\text{turb}}),$$

where F_i represents a single feature in the set **F**. Thus, our Eq. (1) can be rewritten as

$$P(C_{\text{turb}} \,|\, \mathbf{F}) = \frac{P(C_{\text{turb}}) \prod_{i=1}^{N} P(\mathbf{F} \,|\, C_{\text{turb}})}{P(\mathbf{F})}.$$

The potential features included in the Bayesian scheme will be 1) CTC magnitude, 2) the horizontal distance between the CTC and the aircraft, and 3) the vertical distance between the aircraft flight level and the ACHA cloud-top height (CTH) prior to CTC. The authors of this paper do acknowledge the differing vertical coordinate systems between aircraft height (pressure altitude) and ACHA CTH (geopotential altitude). Although this does not allow for an analogous comparison, the Bayesian scheme relies on conditional probabilities of the difference rather than exact figures, and the comparison can continue as long as the coordinate system among the aircraft height and among ACHA CTH remains consistent. We will maintain the pressure-altitude coordinates for the aircraft height and the geopotential coordinates for the ACHA CTH, because these are the natural coordinates for both entities.

For inclusion in the Bayesian scheme, these three features must be statistically different between turbulent cases and nonturbulent cases at the 95% confidence level using a 2-sided Student's *t* test. Since ACHA CTH is used as a potential feature in the Bayesian scheme, pixels that are identified as cirrus or overlapping by the GOES-R ABI cloud-typing algorithm (Pavolonis 2010) will not be used in this analysis. In these cases, ACHA would be identifying the height of the highest cirrus clouds instead of the growing convective cumuliform cloud.

For a given aircraft flight within the radius of uncertainty, three sets of potential features are analyzed (assuming statistical significance). The first set is the largest CTC magnitude and the vertical and horizontal distances between the aircraft and the largest CTC magnitude. The second set is the smallest vertical distance from CTC to aircraft, the horizontal distance between the aircraft and that CTC pixel, and the magnitude of that CTC pixel. The final set is the smallest horizontal distance between the aircraft and CTC, the vertical distance between the aircraft and that CTC pixel, and the magnitude of that CTC pixel. Thus, each time interval will produce three sets of features for analysis. This situation ensures an aircraft that is closer to small-magnitude CTC pixels and farther from large-magnitude CTC pixels is not analyzed the same as an aircraft close to large-magnitude CTC pixels. An aircraft is determined to have experienced LOGT if at least one EDR value is greater than 0.10 for the ICAO standard or a UAL (DAL) EDR value is greater than or equal to 0.10 (0.06) for the PIREP standard. If that occurs, only that segment where the LOGT occurs will be used to assess features.

The probabilistic skill of the Bayesian scheme to predict LOGT will be assessed using the Brier skill score (BSS). The BSS is defined as $\text{BSS} = 1 - B/B_{\text{ref}}$ where

TABLE 4. Relationship between Bayesian probability forecasts and LOGT observations in a 2 × 2 contingency table.

		Obs	
		Yes	No
Forecast	Yes	h	f
	No	m	z

$$B = \frac{1}{k}\sum_{i=1}^{k}[P(C_{\text{turb}} \mid \mathbf{F})_i - O(i)]^2 \quad \text{and}$$

$$B_{\text{ref}} = \frac{1}{k}\sum_{i=1}^{k}[P(C_{\text{turb}}) - O(i)]^2.$$

Here, $O(i)$ represents the occurrence of LOGT, with a value of 1 when LOGT occurs and 0 when it does not occur; k is the total number of aircraft within the radius of uncertainty. The Bayesian scheme is deemed skillful if the BSS is greater than 0, with a perfect score being a BSS equal to 1 (Wilks 2006).

Since LOGT is a yes/no variable, the deterministic skill of the Bayesian scheme can also be assessed using the Pierce skill score (PSS). LOGT will be forecast if the Bayesian probability is higher than the climatology. Like the BSS, the PSS is skillful for values greater than 0 and is perfect for a value of 1. The PSS is equal to the probability of detection (POD: the ratio of the correctly forecast LOGT occurrences to the actual number of LOGT occurrences) minus the probability of false detection (POFD: the number of false alarms divided by the total number of nonoccurrences). The POFD has a negative orientation; therefore, lower values are preferred. A 2 × 2 contingency table, as well as equations for each metric, can be found in Tables 4 and 5, respectively.

TABLE 5. Forecast metrics for the Bayesian probability forecasts using the 2 × 2 contingency table in Table 4.

Forecast metric	Equation
PSS	$\frac{h}{h+m} - \frac{f}{f+z}$
POD	$\frac{h}{h+m}$
POFD	$\frac{f}{f+z}$

4. Results

a. Dependent results

On the basis of the 2008 UAL EDR reports, the climatological probability of LOGT is 3.93%. Of the 738 flight tracks within the radius of uncertainty, only 29 experienced LOGT. Because of the nature of the UAL EDR reports, in increments of $0.1\,\text{m}^{2/3}\,\text{s}^{-1}$ beginning at $0.05\,\text{m}^{2/3}\,\text{s}^{-1}$, the climatology of LOGT is the same for the ICAO and PIREP standard. DAL EDR reports are not used in this metric because of their potentially inconsistent temporal frequency. This low probability is a result of many different factors. One factor is the large area of analysis resulting from *GOES-East* temporal resolution. The area of analysis for an EDR report at ±7 min is approximately 936 km^2. Other potential factors for the low probability are the uncertainty in CTC location, because it takes approximately 4 min for GOES to scan the region of interest, as well as the temporal resolution of *GOES-East*.

Only two features, the magnitude of the CTC and the vertical distance between the aircraft flight level and CTH, are statistically significant at the 95% confidence interval using a 2-sided Student's t test based on the dependent analysis. Therefore, the features used as inputs in the Bayesian scheme will be the highest CTC magnitude, the vertical distance between the aircraft and that CTC pixel, the smallest vertical distance from CTC to aircraft, and the CTC magnitude that is the closest in vertical distance to the aircraft. These features can no longer be assumed to be independent; the Bayesian scheme has been shown to perform well even when independence is violated, however (Domingos and Pazzani 1997).

The conditional probabilities for these features for the ICAO standard can be found in Fig. 3. CTC magnitude and aircraft vertical distance are binned into 2-K and 2000-ft boxes, respectively. These conditional probabilities have been smoothed using a nine-point running boxcar average.

Figure 3a shows the conditional probability of turbulence with respect to CTC magnitude for the ICAO standard. For higher CTC magnitudes [less than $-16\,\text{K}\,(15\,\text{min})^{-1}$], the conditional probability of LOGT exceeds the conditional probability of no turbulence. The same configuration exists for the PIREP standard (not shown). CTC magnitude represents the vertical growth of the cloud (Sieglaff et al. 2011), with higher CTC magnitude representing more rapid vertical growth. It is assumed that this vertical growth is the result of upward vertical velocity (Adler and Fenn 1979; Glass and Carlson 1963), which is a known cause of aircraft turbulence (Sharman et al. 2006).

The conditional probability for the aircraft vertical distance from the CTC for the ICAO standard can be seen in Fig. 3b. Vertical distances of less than zero represent an aircraft flight level that is below the CTH. Higher conditional probability of LOGT exists at these distances, potentially a result of aircraft flying through

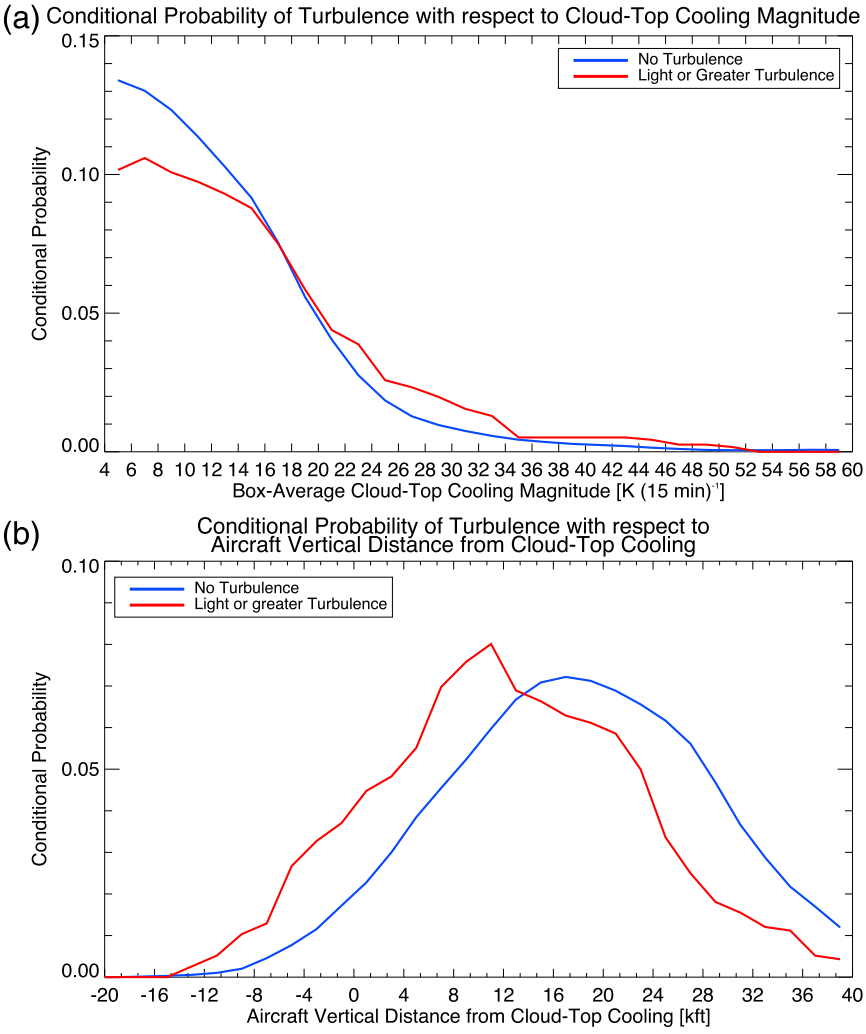

FIG. 3. (a) Conditional probability of turbulence with respect to CTC magnitude for the ICAO standard of LOGT for EDR values of >0.1. The conditional probability of turbulence exceeds the conditional probability of no turbulence when the CTC magnitude is less than $-16\,\mathrm{K}\,(15\,\mathrm{min})^{-1}$, a result of greater upward vertical velocity. (b) Conditional probability of turbulence with respect to aircraft vertical distance from cloud-top height for the ICAO standard of LOGT for EDR values of >0.1. Distances of less than zero represent an aircraft flight level that is below the cloud-top height in geopotential coordinates.

intense upward vertical motions. Aircraft just above the CTH also have a greater conditional probability of LOGT in comparison with no turbulence. This is consistent with Lane et al. (2012), who indicated that the risk of moderate turbulence is 10 times as great for aircraft within 12 000 feet of the Next-Generation Radar echo top. Since the CTH represents the height of the cloud prior to CTC, it is possible that these aircraft are also potentially flying through intense upward vertical motions as the cloud grows. Another potential reason is vertical gravity waves that are excited by the growing cloud (Alexander et al. 1995; Hung et al. 1980), which is another known cause of observed turbulence (Bedard et al. 1986; Lane et al. 2012). Again, the same conditional probability pattern exists for the PIREP standard (not shown) as for the ICAO standard that is seen in Fig. 3b.

b. *Independent results*

Using the conditional probabilities of turbulence represented by Fig. 3, the probability of LOGT for the independent dataset from 2011 is predicted using the Bayesian scheme. With a BSS of 0.032 (0.174) for the ICAO standard (PIREP standard), the Bayesian scheme is skillful at predicting LOGT in the vicinity of CTC when compared with climatology alone. The

difference in the BSS between the ICAO standard and PIREP standard is due to 13 EDR reports in the independent dataset that are considered to be LOGT by the PIREP standard but not by the ICAO standard. When using the ICAO standard conditional probabilities, these 13 EDR reports have an average Bayesian probability of 16.0%. This is higher than the climatological probability of LOGT, and thus the forecast skill of the Bayesian scheme is reduced when they are not considered to be LOGT. Using the ICAO standard conditional probabilities in Fig. 3 from the dependent dataset but including these 13 EDR reports from the independent dataset to be considered as LOGT increases the ICAO standard BSS to 0.141. The PSS for the Bayesian scheme is also skillful at 0.284 (0.283) for the ICAO standard (PIREP standard).

The impact of the Bayesian scheme on turbulence prediction can be seen in Fig. 4. For instances in which ICAO standard (PIREP standard) LOGT does not occur, 64.3% (69.1%) had a Bayesian probability that was lower than the climatology. For instances in which ICAO standard (PIREP standard) LOGT does occur, 64.0% (59.3%) have an increased probability relative to climatology.

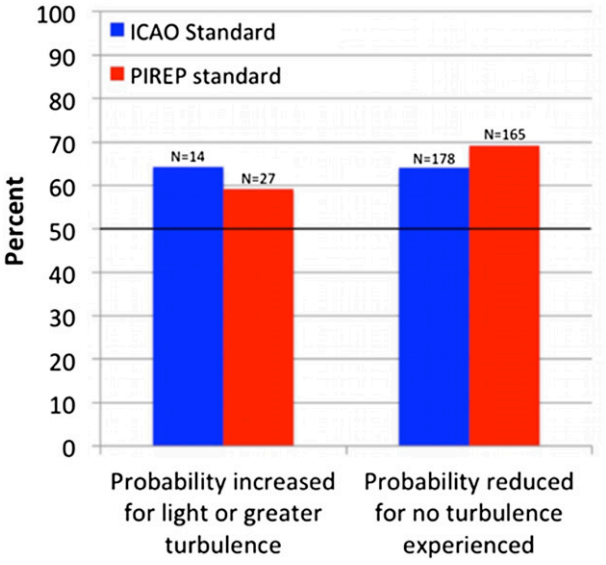

FIG. 4. Percent of improved forecasts when using the Bayesian scheme in comparison with climatology alone. For the ICAO standard of LOGT for EDR values of >0.1, the Bayesian scheme increased (decreased) the probability of turbulence for 64.3% (64.0%) of instances in which turbulence does (does not) occur. For the PIREP standard of LOGT for EDR values of ≥0.06, the Bayesian scheme increased (decreased) the probability of turbulence for 59.3% (69.1%) of instances in which turbulence does (does not) occur.

5. Summary and conclusions

This study uses a satellite-based cloud-top cooling (UW-CTC) algorithm to identify the probability of convectively induced aircraft turbulence in the vicinity of a cloud exhibiting a UW-CTC rate. The overall probability of turbulence around CTC is low, with only 3.93% of 738 Boeing 737s and 757s from 2008 experiencing light or greater turbulence. When using a Bayesian scheme, the skill of predicting convectively induced turbulence is increased when compared with predicting turbulence on the basis of climatology alone. This result indicates that knowledge of the CTC magnitude, as well as the spatial proximity between the aircraft and CTC, increases turbulence predictability. Light-or-greater turbulence is associated with CTC magnitudes of greater than or equal to $-16\,\mathrm{K}\,(15\,\mathrm{min})^{-1}$. Aircraft with flight levels below 8000 ft above the cloud height also have a higher conditional probability of LOGT than of no turbulence.

While the overall probability of LOGT is low with respect to CTC, the Bayesian scheme model can be used in conjunction with other satellite turbulence predictors to create a global turbulence probability product. Initial plans include combining the CTC turbulence probabilities with turbulence probabilities associated with mountain waves, transverse banding, tropopause folds, and overshooting tops.

Acknowledgments. This research is supported by GOES-R Proving Ground grant and GIMPAP Contract NA10NES4400013. The authors thank two anonymous reviewers for their contributions to this manuscript.

REFERENCES

Adler, R. F., and D. D. Fenn, 1979: Thunderstorm intensity as determined from satellite data. *J. Appl. Meteor.,* **18,** 502–517.

Alexander, M. J., J. R. Holton, and D. R. Durran, 1995: The gravity wave response above deep convection in a squall line simulation. *J. Atmos. Sci.,* **52,** 2212–2226.

Bedard, A. J., F. Canavero, and F. Einaudi, 1986: Atmospheric gravity waves and aircraft turbulence encounters. *J. Atmos. Sci.,* **43,** 2838–2844.

Cornman, L. B., C. S. Morse, and G. Cunning, 1995: Real-time estimation of atmospheric turbulence severity from in-situ aircraft measurements. *J. Aircr.,* **32,** 171–177.

——, G. Meymaris, and M. Limber, 2004a: An update on the FAA Aviation Weather Research Program's in situ turbulence measurement and reporting system. *Proc. 11th Conf. of Aviation, Range, and Aerospace Meteorology,* Hyannis, MA, Amer. Meteor. Soc., P4.3. [Available online at https://ams.confex.com/ams/pdfpapers/81622.pdf.]

——, P. Schaffner, C. A. Grainger, R. T. Neece, T. S. Daniels, and J. J. Murray, 2004b: Eddy dissipation rate performance of the Tropospheric Airborne Meteorological Data Reporting (TAMDAR) sensor during the 2003 Atlantic THORPEX regional campaign. Abstract, *11th Conf. on Aviation, Range,*

and Aerospace Meteorology, Hyannis, MA, Amer. Meteor. Soc., P4.13. [Available online at https://ams.confex.com/ams/11aram22sls/webprogram/Paper81770.html.]

Domingos, P., and M. Pazzani, 1997: Beyond independence: Conditions for the optimality of the simple Bayesian classifier. *Mach. Learn.,* **29,** 103–130.

Glass, M., and T. N. Carlson, 1963: The growth characteristics of small cumulus clouds. *J. Atmos. Sci.,* **20,** 397–406.

Glickman, T., Ed., 2000: *Glossary of Meteorology.* 2nd ed. Amer. Meteor. Soc., 855 pp.

Hamilton, D. W., and F. H. Proctor, 2002: Convectively induced turbulence encountered during NASA's fall-2000 flight experiments. *Extended Abstracts, 10th Conf. on Aviation, Range, and Aerospace Meteorology,* Portland, OR, Amer. Meteor. Soc., 10.8. [Available online at https://ams.confex.com/ams/pdfpapers/40038.pdf.]

Heidinger, A. K., 2011: ABI cloud height. NOAA NESDIS Center for Satellite Applications and Research Algorithm Theoretical Basis Doc., 77 pp. [Available online at http://www.goes-r.gov/products/ATBDs/baseline/Cloud_CldHeight_v2.0_no_color.pdf.]

Hung, R. J., T. Phan, D. C. Lin, R. E. Smith, R. R. Jayroe, and S. West, 1980: Gravity waves and GOES IR data study of an isolated tornadic storm on 29 May 1977. *Mon. Wea. Rev.,* **108,** 456–464.

International Civil Aviation Organization, 2007: Meteorological service for international air navigation. 16th ed. ICAO Rep., 185 pp. [Available online at http://www.wmo.int/pages/prog/www/ISS/Meetings/CT-MTDCF-ET-DRC_Geneva2008/Annex3_16ed.pdf.]

Kaplan, M. L., A. W. Huffman, K. M. Lux, J. J. Charney, A. J. Riordan, and Y.-L. Lin, 2005: Characterizing the severe turbulence environments associated with commercial aviation accidents. Part 1: A 44-case study synoptic observational analyses. *Meteor. Atmos. Phys.,* **88,** 129–153.

Kossin, J. P., and M. Sitkowski, 2009: An objective model for identifying secondary eyewall formation in hurricanes. *Mon. Wea. Rev.,* **137,** 876–892.

Lane, T. P., R. D. Sharman, St. B. Trier, R. G. Fovell, and J. K. Williams, 2012: Recent advances in the understanding of near-cloud turbulence. *Bull. Amer. Meteor. Soc.,* **93,** 499–515.

Mecikalski, J. R., and Coauthors, 2007: Aviation applications for satellite-based observations of cloud properties, convective initiation, in-flight icing, turbulence, and volcanic ash. *Bull. Amer. Meteor. Soc.,* **88,** 1589–1607.

Meymaris, G. and R. Sharman, 2013: NCAR in situ vertical winds-based EDR estimation algorithm description, version 0.9. University Corporation for Atmospheric Research Draft Rep., 20 pp. [Available online at http://www.ral.ucar.edu/projects/in_situ_software/insitu_description_report.pdf.]

Murray, J. J., 2002: Aviation weather applications of Earth Science Enterprise data. *Earth Obs. Mag.,* **11,** 26–30.

Pavolonis, M. J., 2010: GOES-R Advanced Baseline Imager (ABI) algorithm theoretical basis document for cloud type and cloud phase, version 2.0. NOAA NESDIS Center for Satellite Applications and Research Algorithm Theoretical Basis Doc., 86 pp. [Available online at http://www.star.nesdis.noaa.gov/goesr/docs/ATBD/Cloud_Phase.pdf.]

Pearson, J. M., and R. Sharman, 2013: Calibration of in situ eddy dissipation rate (EDR) severity thresholds based on comparisons to turbulence pilot reports (PIREPs). Abstract and Recorded Presentation, *16th Conf. on Aviation, Range, and Aerospace Meteorology*, Austin, TX, Amer. Meteor. Soc., 6.1. [Available online at https://ams.confex.com/ams/93Annual/webprogram/Paper219281.html.]

Schwartz, B., 1996: The quantitative use of PIREPs in developing aviation weather guidance products. *Wea. Forecasting,* **11,** 372–384.

Sharman, R., C. Tebaldi, G. Wiener, and J. Wolff, 2006: An integrated approach to mid- and upper-level turbulence forecasting. *Wea. Forecasting,* **21,** 268–287.

Sieglaff, J. M., L. M. Cronce, W. F. Feltz, K. M. Bedka, M. J. Pavolonis, and A. K. Heidinger, 2011: Nowcasting convective storm initiation using satellite-based box-averaged cloud-top cooling and cloud-type trends. *J. Appl. Meteor. Climatol.,* **50,** 110–126.

——, D. C. Hartung, W. F. Feltz, L. M. Cronce, and V. Lakshmanan, 2013: A satellite-based convective cloud object-tracking and multipurpose data fusion tool with application to developing convection. *J. Atmos. Oceanic Technol.,* **30,** 510–525.

Walther, A., and A. K. Heidinger, 2012: Implementation of the daytime cloud optical and microphysical properties algorithm (DCOMP) in PATMOS-x. *J. Appl. Meteor. Climatol.,* **51,** 1371–1390.

Wilks, D. S., 2006: *Statistical Methods in the Atmospheric Sciences.* 2nd ed. Academic Press, 627 pp.